

# Description and Simulation Results for a GNSS Signal-Based Navigation System for a Mission to the Moon

M. Manzano, J. Alegre, A. Pellacani, *GMV Spain*  
G. Seco, J. López, E. Guerrero, *UAB, Spain*  
A. García, *ESA/ESTEC, The Netherlands*

## BIOGRAPHY

**María Manzano** received a Master of Science in Mathematics in 2001 from the Complutense University of Madrid, Spain. Since then she has worked in GMV, especially in GNSS related projects, such as GNSS PVT navigation algorithms, GPS and GALILEO, separate or combined GNSS systems navigation, modernized GNSS signals, absolute and relative navigation, pseudorange and carrier phase based positioning, attitude and attitude rate computation, post-processing and real time, simulated and real data, ground and spatial applications, GNSS receiver simulators, signal characterization, and GNSS hybridization with other sensors.

**Julia Alegre-Rubio** received the M.Sc. in Telecommunication Engineering from the Polytechnic University of Madrid (2007) and also the Master in Space Technology (2009). She works in GMV on signal processing for GNSS receivers, GNSS performance verification, modernized GNSS signals, GPS and GALILEO, focused on Public Regulated Service (PRS). She has held several positions in Hispasat, National Institute of Aerospace Technology and ESA.

**Andrea Pellacani** received a Master of Science in Aerospace engineering in 2011 from the University of Bologna, Italy. Since then he has worked in GMV, especially in GNC related projects, such as Lunar Lander project for the development of autonomous descent and landing algorithms, iGNC for the implementation of an attitude guidance, COBRA and ANDROID for debris removals using chemical thruster plume impingement and net system. He has also had experience related to mission analysis and navigation algorithms for the GNSS hybridization with other sensors using an Extended Kalman Filter.

**Gonzalo Seco-Granados** received the M.Sc. and Ph.D. degrees in Telecommunication Engineering in 1996 and 2000, respectively, from Universitat Politècnica de Catalunya (UPC). He also received an MBA from IESE, University of Navarra, Barcelona, in 2002. From 2002 to 2005, he was member of the technical staff at the

European Space Research and Technology Center (ESTEC), European Space Agency (ESA), Noordwijk, The Netherlands, involved in the Galileo project and leading the activities on indoor GNSS. Since 2006, he is Associate Professor at the Department of Telecommunications and Systems Engineering, Universitat Autònoma de Barcelona (UAB), and member of the Signal Processing for Communications and Navigation (SPCOMNAV) group. Gonzalo Seco-Granados has authored over 150 technical papers and has been principal investigator of over 25 research projects.

**José A. López-Salcedo** received the M.Sc. and Ph.D. degrees in Telecommunication Engineering in 2001 and 2007, respectively, from Universitat Politècnica de Catalunya (UPC). From 2002 to 2006, he was a Research Assistant at UPC involved in R+D projects related with synchronization techniques for digital receivers, satellite communications and iterative decoding techniques for MIMO wireless systems, both for private industry and public administrations. Since 2006, he is Assistant Professor, and Associate Professor since 2013 at the Department of Telecommunications and Systems Engineering, Universitat Autònoma de Barcelona (UAB), and member of the SPCOMNAV group. He has been UAB principal investigator for the ROCAT and ADAPT projects of the European Space Agency.

**Enric Guerrero Rubio** received the M.Sc. degrees in Telecommunication Engineering in 2013 from Universitat Autònoma de Barcelona (UAB). During his final degree project he participated in the "Moon-GNSS: Weak GNSS Signal Navigation on the Moon". In October 2013, he joined UAB as project engineer located at the European Space Research and Technology Center (ESTEC), The Netherlands, working on the testing of Galileo receivers and hybrid navigation.

**Alberto Garcia-Rodriguez** works in the radio navigation section in ESA. He is involved in activities related to GNSS space receivers and applications. He worked previously at GMV (Spain) for several GNSS navigation projects. He has an MSc in Telecommunications Engineering from the Polytechnic Uni. of Madrid (1992).

## ABSTRACT

If weak-signal GNSS navigation were possible in future lunar exploration missions, this would increase the robustness of the navigation during all mission phases and improve its autonomy. The Moon mission scenario is very challenging for the GNSS signals acquisition. Due to the large propagation distances, the GNSS signal arrives to the spacecraft with low C/N0 values. This way, the main requirements of the GNSS receiver are imposed by the low C/N0 GNSS signals that need to be acquired.

In the frame of a European Space Agency (ESA) activity, the objective of the Moon-GNSS study has been to determine the feasibility using weak-signal GNSS (GPS/Galileo) technology in future lunar exploration missions, to improve the navigation performance in terms of accuracy, cost reduction, robustness and autonomy. During the Moon-GNSS activity, the analysis and the identification of the Moon-GNSS navigation receiver requirements for the upcoming lunar exploration missions have been performed. The main objective of the Moon-GNSS analysis has been to characterize the GNSS signals arriving to the spacecraft, especially at the vicinity of the Moon.

A Proof-of-Concept (PoC) demonstrator of the weak-signal Moon-GNSS navigation has been designed and implemented, showing the main functional and performance capabilities of the Moon-GNSS receiver.

A test campaign representative of a real Moon-GNSS mission has been performed, covering all the mission phases representative of the real mission conditions in terms of dynamics and signal disturbances. This study has carefully analyzed all the test cases that were considered interesting in order to evaluate the standard (that considers only the nominal sensors for a Lunar mission, but not GNSS), the hybrid (nominal sensors and also GNSS), and stand-alone GNSS navigation performances.

## MOON-GNSS SCENARIO DEFINITION AND ANALYSIS

### Moon-GNSS scenario definition

In order to analyze and identify, for the upcoming lunar exploration missions, the Moon-GNSS navigation receiver requirements, the first task has been to define the Moon-GNSS scenario to be used as reference for the GNSS receiver and the later hybridization with other sensors. The selected Moon-GNSS reference scenario is based on the ESA Lunar Lander mission, with landing site near Moon's South Pole. The different phases of the Moon-GNSS reference trajectory are listed below:

- Phase 1 - LTO (Lunar Transfer Orbit). This is the phase that starts from a LEO and finishes when the Spacecraft is captured by the Moon gravity;
- Phase 2/3/4 - ORB1/2/3. These phases (orbit around the Moon) contain all the maneuvers to reach the LLO;

- Phase 5 - ORB4 or LLO (Low Lunar Orbit). During this phase the Spacecraft orbits around the Moon on fixed altitude orbit of 100 km;
- Phase 6 - COASTING. The approach to the Moon surface starts. In this phase the Spacecraft is in an elliptical orbit of 15x100 km;
- Phase 7 - D&L (Descent and Landing). The final descent, from 15 km altitude to the Landing Site (see Fig. 1);
- Phase 8 - SO (Surface Operations). This phase simulates a static surface operation, with the rover 500 m from the Lander (which is in the Landing Site).

Another trajectory composed with similar phases but arriving at an inclination of 30° and landing close to 25° N latitude has also been analysed to assess the influence of the orbit inclination and the arrival conditions on the GNSS navigation.

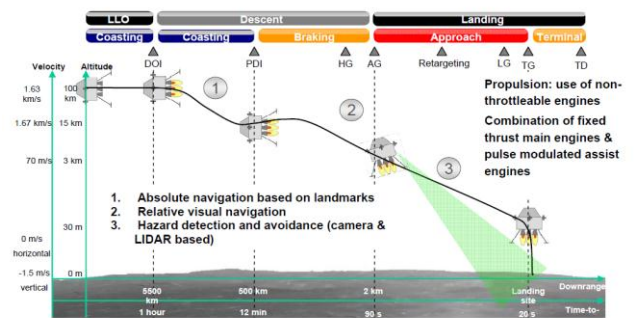


Fig. 1: LLO and Descent and Landing representation obtained from [1]

### Moon-GNSS scenario analysis set-up

An extensive Moon-GNSS scenario analysis has been performed in order to provide with the due inputs for the derivation of the Moon-GNSS navigation receiver requirements, and for the definition of the GNSS receiver module architecture and algorithms (weak signal processing, filtering and navigation). The following aspects have been used in the analysis:

- All the different phases of the Moon-GNSS S/C trajectory have been analyzed.
- GPS 27-Satellite Constellation and Galileo 24-Satellite Constellation have been considered.
- A Moon GNSS-like (MGNSS) signal orbiting around the Moon has also been considered for all the phases of the trajectory. The optimum MGNSS constellation has been analyzed, to improve the geometric conditions of the arriving signals and to avoid/minimize the near-far effect.
- Depending on the date, the relative geometry between the GPS/Galileo constellations and the Spacecraft changes, thus, imposing different requirements and affecting the performances of the Moon-GNSS system. The date has also an important impact on the SC attitude, in order to respect specific constraints related with FoV of sensors, pointing direction of the main engines and position

of the solar panels on the Spacecraft, and in order to select the most suitable location of the GNSS antenna(s) during the different phases of the Moon-GNSS reference trajectory. For this analysis, it has been considered the 19 February 2019.

- L1 and L5 frequencies are analyzed both for GPS and Galileo
- Specific on-board antenna patterns in GPS and Galileo have been considered for both L1 and L5 frequencies.
- Different receiver antenna types and antenna gains have been considered, specific for both L1 and L5: no receiver gain, low gain and different high gains.

The analysis procedure steps include:

- Updated power link budget model to cover distances up to the Moon.
- Analysis of theoretical visibility (main and first side lobes of the current GPS and Galileo constellation satellites, see Fig. 2) for different transfer orbit positions.
- Power Link budget analysis of “visible” signals (see Fig. 3).

starting positions of the GNSS constellations. This way, the system has been analyzed for every possible position of the GPS and Galileo constellations, and for different arrival directions of the GNSS signal to the Spacecraft, providing very useful statistical results.

The following magnitudes have been analyzed:

- GDOP: Geometric Dilution of Precision. In an only-GNSS-Rx configuration, the GDOP provides a direct reference of the achievable navigation estimation accuracy for instantaneous (non-recursive) estimation (where at least 4 GPS/Galileo signals are required). For a recursive solution (e.g. Kalman filter with an orbit propagator model) and with or without the use of other sensors, the estimation accuracy can be significantly improved but the GDOP is still a good indicator for relative comparison on the achievable accuracy in different points/phases of the Moon-GNSS scenario.
- GNSS signal strength in different points/phases of the Moon-GNSS scenario.
- Direction of the different GPS/Galileo signals arriving to the Spacecraft. Since the GPS/Galileo satellites will be at far distances from the Moon-GNSS receiver, it is expected that all the signals will be concentrated in a relatively small area of the GNSS antenna sky. On one side, this will strongly penalize the GDOP but, on the other side, it may allow the use of GNSS high-gain antennas (much more directional than normal GNSS antennas).

The LTO phase starts at about 1000 km height over the Earth surface and finish at about 200 km height over the Moon. Although all the different phases of the Moon-GNSS S/C trajectory have been analyzed, the LTO phase provides very interesting results to derive the Moon-GNSS navigation receiver requirements. Some examples of the obtained results during the LTO phase are presented below:

- Using randomized simulations, it has been analyzed the probability of acquiring 1, 2, 4 or more GPS and Galileo signals as function of the SC distance to Earth and the receiver C/No acquisition/tracking thresholds. Fig. 4 shows the results obtained for a high gain antenna and L1 frequency. The main conclusion is that the worst situation happens at the Moon vicinity (as expected due to the free space loss). The required GNSS-Rx acquisition/tracking sensitivity for a high gain antenna is over 10 dB- Hz for 5 or more GPS/Galileo signals for 99% of the time.
- It has also been analyzed the number of GPS or Galileo signals coming from the antenna main or secondary lobes for different CN0 thresholds (0, 10 and 20 dBHz). Fig. 5 shows that most of the signals are received from the secondary lobes, and the number of signals coming from the main lobe is very low (1 or 2). Besides, the results showed that using a

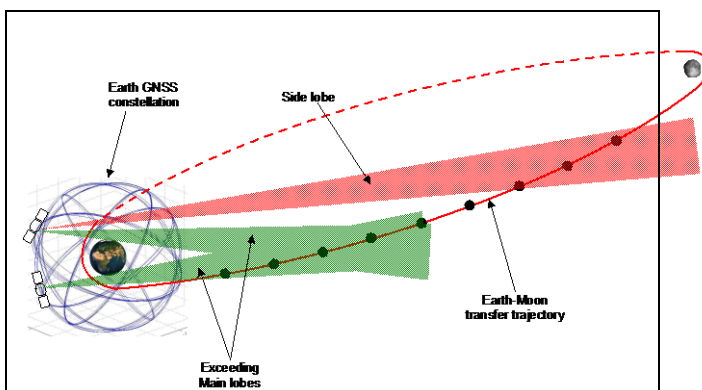


**Fig. 2 Geometrical visibility of main radiation lobe (out of Earth umbra) and side lobes**

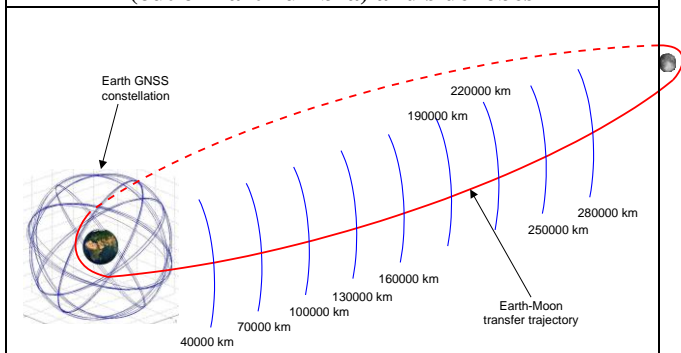


**Fig. 3 C/No link budget analysis at several distances over the Earth-Moon transfer orbit**

### Moon-GNSS scenario analysis results

Two different types of analysis have been performed:

- Deterministic case (1 run) where the GNSS satellites position correspond to the selected date;
- A randomized case (multiple runs) where the GPS and Galileo link budgets are calculated for different

high gain receiver antenna the number of GPS + Galileo signals with  $C/N_0 > 10\text{dBHz}$  is greater than 4, even at the vicinity of the Moon.

- Using a deterministic case, where the GNSS satellites position correspond to the selected date, Fig. 6 shows the obtained GPS link budget ( $C/N_0$ ) for a high gain receiving antenna. As expected, the received signal power decreases with distance. Some higher “peaks” are observed, corresponding to signals coming from the main lobe of the transmitting antennas, and the figure is “thicker” with lower  $C/N_0$ s, since most of the signals are received from the secondary lobes.
- DOP values grow up to a value of hundreds ( $\sim 100$  times higher than normal Earth values) at the vicinity of the Moon. The worst value of DOP is the VDOP (projection on the SC to Earth direction).
- For the selection of the optimum number, location and type of antenna to be used, the angle of the arriving signals is analyzed. The optimum arriving angle is close to 0 degrees (antenna boresight, maximum gain). Fig. 7 shows the angle of the arriving signals, for three different phases and three different locations of the antenna.

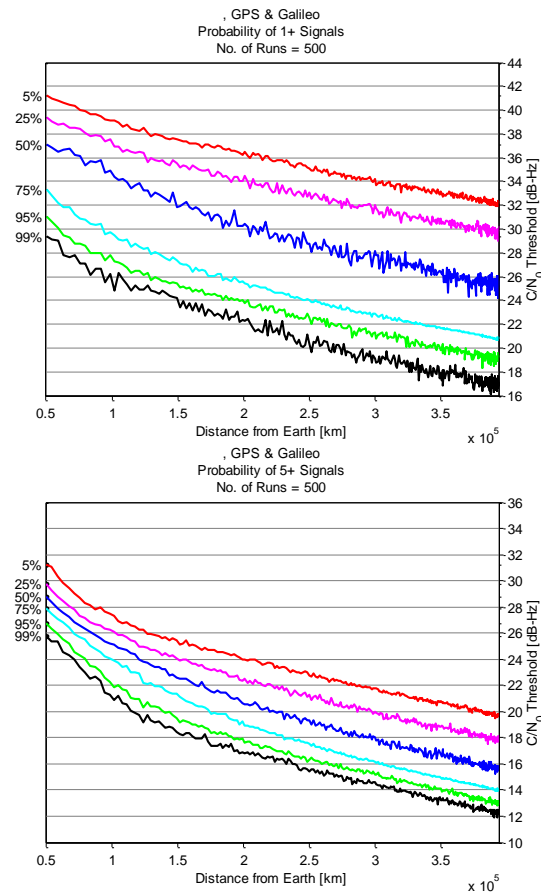


**Fig. 4** Probability of acquiring 1 or more (left) and 5 or more (right) GPS and Galileo signals as function of the SC distance to Earth and the receiver  $C/N_0$  acquisition/tracking thresholds. High receiver gain is considered. L1 frequency.

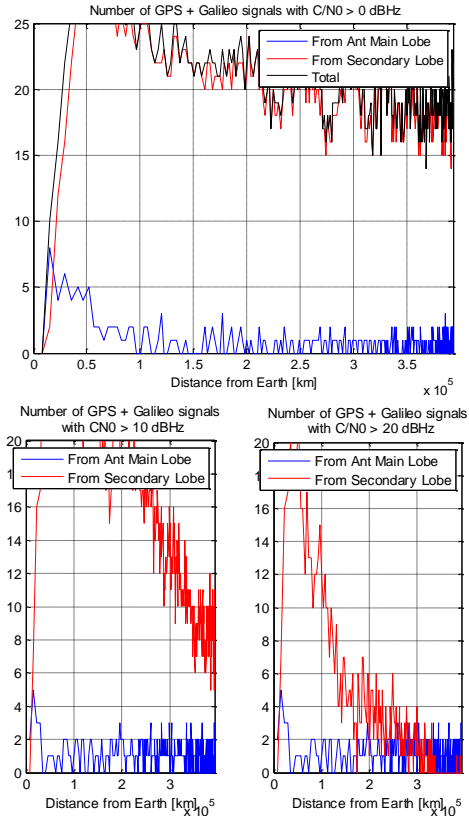


**Fig. 5** Number of GPS + Galileo signals from antenna main and secondary lobes

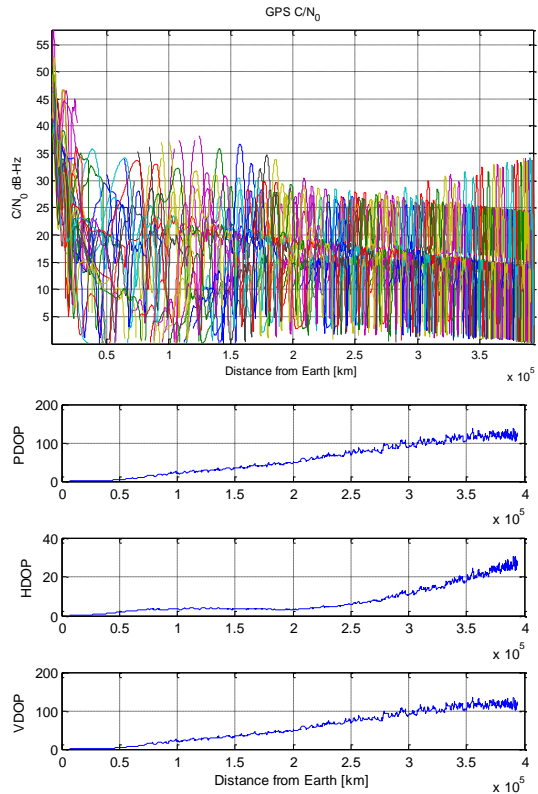


**Fig. 6:** GPS  $C/N_0$ s values (left), PDOP, HDOP, VDOP (the vertical direction is the Earth pointing direction) (right)

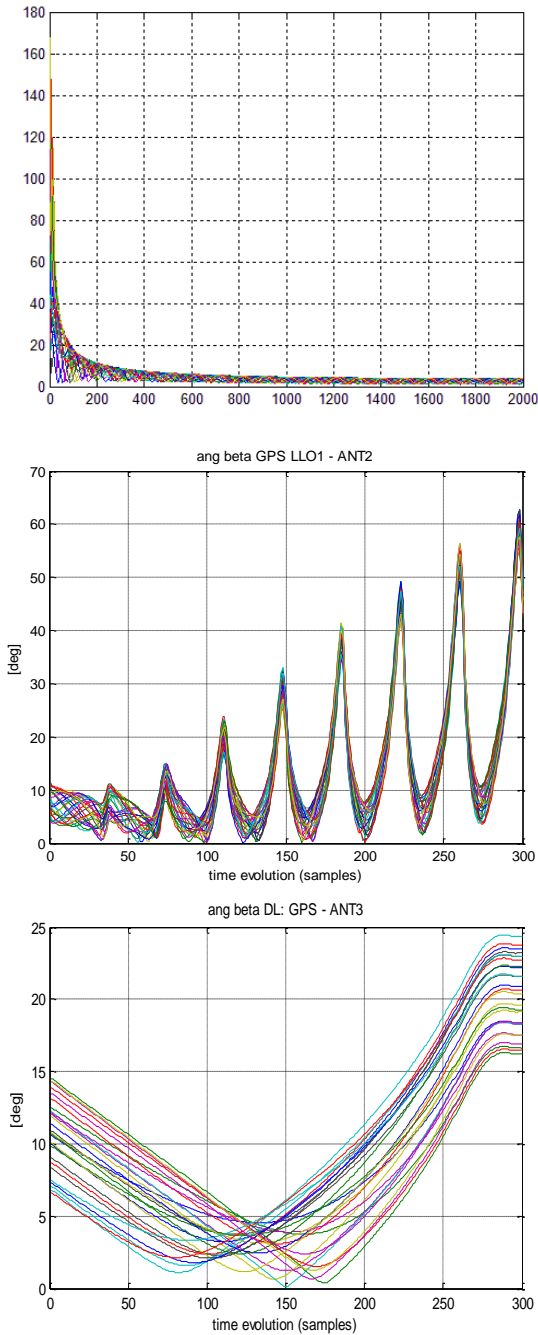


**Fig. 7: Angle formed by the antenna pointing and the S/C to EGNSS satellites for three different antenna locations: LTO phase, antenna 1 (left); ORB1 phase, antenna 2 (middle), D&L phase, antenna 3 (left).**

The main objective of the Moon-GNSS analysis has been to characterize the GNSS signals arriving to the S/C, especially at the vicinity of the Moon. From this analysis, the following conclusions have been derived:

- Reaching values of C/N0 down to 15dBHz is feasible. The range 10 to 15 dBHz is challenging, and going below 10 dBHz is very complicated because it requires very long coherent correlations (around 500 ms). 10 dBHz is the frontier between a very challenging problem and what starts to be unfeasible.

- The results may be improved in the sense of reaching lower values of C/N0 using more sophisticated approaches, such a drastic reduction of the window search and relaxing a bit the detection and false alarm probabilities. In that case, it may be possible to approach 5 dBHz. But going below 5 dBHz seems unfeasible (unless complex tight coupling with inertial sensors is included).
- In any case, performing long coherent correlations is mandatory, so we should use pilot signals always. The use of data components involves a too strong limitation.
- If the chip rate and the receiver bandwidth increase, the code phase accuracy clearly improves for a given C/N0, but the C/N0 lower limit until which a given receiver can be reliably used does not improve. The only way to lower the threshold is to increase the coherent correlation interval and to reduce the uncertainty window. Likewise, the use of BOC signals improves a bit the accuracy (e.g. in a factor 1.5 for BOC(1,1) approx.), but does not change the threshold.
- In this sense, the selection and location of the antenna(s) can improve significantly the obtained results, and this depends strongly on the specific selected Moon GNSS reference trajectory attitude for the different phases. Two main issues have been analyzed in order to maximize the number and quality of arriving signals:
  - i. First, the number and location of the GNSS antenna(s) within the Spacecraft,
  - ii. Second, the antenna(s) type.
- Soon after the Lunar Lander spacecraft goes above the GNSS constellations, the directions of arrival of the incoming signals are within a narrow portion of the GNSS receiving antenna sky. In particular, this allows the use of a narrow high-gain pattern antenna during the LTO.
- After a thorough analysis of the most suitable location and type of antenna(s), taking into account the maximum antenna size allowed by the spacecraft dimension limits, three antenna locations have been considered, with different antenna types each. As a conclusion of the analysis, these three locations for the GNSS receiving antenna are the ones with more visibility during the different phases of the Moon-GNSS S/C trajectory.
- Most of the signals are received from the secondary lobes of the transmitter antennas, and the number of signals coming from the main lobe is very low (1 or 2).
- The DOP values grow up to a value of hundreds (~100 times higher than normal Earth values) at the vicinity of the Moon.
- In the Moon-GNSS scenario, the portion of the ionosphere will be crossed at low elevations and the ionospheric delay can achieve high values. On the other hand, in the Moon-GNSS study only signals coming from the main transmitter antenna lobes go through the ionosphere, and the number of signals

coming from the main lobe is very low (1 or 2). Considering that a model can compensate for 50% - 75% of the ionospheric delay, taking into account the code standard deviation due to coherent integration at low C/N0 values and the very high DOP values, the conclusion is that ionospheric effect is not the main determinant of the accuracy and dual frequency processing is not necessary; and that applying a model to compensate for ionospheric delay would be enough.

## MOON GNSS RECEIVER MODULE REQUIREMENTS

The impact of the receiver requirements on the Moon-GNSS receiver module architecture and algorithms has been analyzed. The main requirements of the receiver are imposed by the low C/N0 GNSS signals that need to be acquired. For this purpose, the following aspects of the GNSS receiver have been analysed:

- Front-end requirements: High quality and shielded low noise Front End (FE) is required to receive weak low C/No signals and to avoid interferences from the surrounding equipment. Some examples of Front Ends space qualified have been reviewed.
- Clock reference requirements: High stability local oscillator is required to support several seconds of long coherent and non-coherent integration times during weak signal high sensitivity processing. A review of the different existing oscillators has been performed.
- Memory requirements: Regarding the raw data logging, the platform must be able to record and store several seconds of raw data (coming from the GPS/Galileo RF Front-end) for long coherent and non-coherent correlation integrations. Besides, the proposed algorithms require a high amount of data management and heavy calculations. To avoid out of memory problems, a minimum of RAM is also required.
- Antenna requirements: Regarding the antenna requirements, the main issues are to maximize the number and quality of arriving signals. This strongly depends on the Spacecraft trajectory and attitude.

Another important aspect is the selection architecture of the GNSS receiver module. The architecture of the receiver is based on an open-loop configuration that generates the code-phase and frequency estimates. It has been implemented to be compatible with GPS and Galileo signals, both with pilot and data components. Furthermore, it was designed to achieve the low levels of sensitivity required for indoor applications. It is based on the ESA patented “Double-FFT Method” for an efficient implementation all these techniques [5]. Besides, the receiver can use assistance information to limit the time-frequency search range and it does not need to integrate the measurements of the INS at a signal level.

## PROOF OF CONCEPT DESCRIPTION

A Proof-of-Concept (PoC) demonstrator of the weak-signal Moon-GNSS navigation has been designed and implemented, to show the main functional and performance capabilities of the Moon-GNSS receiver. The PoC is a simulator developed in Matlab/Simulink and composed by three different modules (Fig. 8):

- Scenario Generator Module (SGM): This module is in charge of simulating the scenario characteristics and the received GNSS signals values (GNSS constellations, S/C dynamics for the different scenario phases, relative geometry between the GNSS constellations and S/C, Earth and Moon signal occultation, direction of the different GNSS signals arriving to the S/C, visibility and power link budget).
- GNSS Receiver Module (GRM): This block implements a Raw Observable Generator (ROG) whose main objective is to generate fractional pseudoranges and frequency observables with the same performance as a real receiver, taking as input the results from the SGM.
- Navigation Filter Module (NFM): This module is in charge of implementing a navigation filter taking as inputs the GNSS Receiver Module observables (pseudoranges and frequency observables) and the outputs from the different sensors used in every phase of the mission.

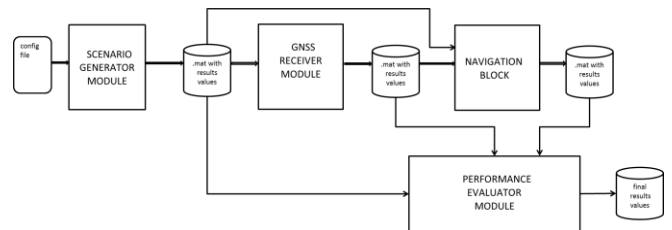


Fig. 8: Proof of Concept architecture

The Performance Evaluator Module (PEM) is in charge of the post processing of the data for the results generation. The outputs of the three modules (SGM, GRM and NFM) are used to obtain final results, different statistics and graphics. The PoC allows the user the configuration/selection of multiple parameters for all the different modules, sequential execution of several tests, generation of plots and storing the results.

### Scenario Generation Module (SGM)

The Scenario Generation Module is in charge of simulating the scenario characteristics and the received signals values. Its main output results are:

- Range distance from the spacecraft to the different navigation satellites;
- Doppler expected values in the GNSS signals in reception;
- C/N0 values of the GNSS signals reaching the spacecraft.

To obtain all these results, the simulator implements orbit propagators, attitude determination, link budget calculations, and antenna radiation diagrams. The main processing functions are:

- Load the SC position, velocity and attitude (time evolution);
- Propagate the GNSS positions (for the GPS, Galileo and MGNSS constellations);
- Calculate the true ranges, considering the Earth and Moon blinding (occultation);
- Calculate the received power, considering the transmitting and receiving antenna gains, and the free space losses;
- Calculate the pseudoranges, including clock errors, ionospheric delay and ephemeris errors.

For the calculation of the power from the Navigation Systems (C/N0) that would arrive to an on-board SC receiver, the following effects are taken into account: the Earth and Moon blinding occultation, the transmission and receiver gains, free-space losses, atmospheric and other losses, etc. The updated power link budget model to cover distances up to the Moon is based on the following formulation:

$$C/N_0 = EIRP + G_{rx} + FLS + L_I + L_{Nf} + T_n - K_b \quad (\text{Eq. 1})$$

Where:

Param.	Description	Value
EIRP	GPS satellites Effective Isotropic Radiated Power	From EIRP vs boresight pattern
$G_{rx}$	Gain of the receiving antenna in the GPS satellite direction, function of the off-nadir angle and of the antenna pattern	From gain pattern
FLS	Free Space Loss. Attenuation of signal travelling a distance R computed as $20 \cdot \log_{10}(\lambda / (4 \cdot \pi \cdot R))$ , with $\lambda = 0.1903$ m at L1 wavelength, $\lambda = 0.2548$ m at L5 wavelength	$20 \log(\lambda / 4\pi R)$ , where R is the distance and $\lambda$ is the L1/L5 wavelength
$L_I$	Implementation, A/D conversion losses	[dBs] (1-bit or 3-bit digitalization)
$L_{Nf}$	Noise figure of receiver/front end	[dBs]
$T_n$	Noise temperature loss computed as $10 \cdot \log_{10}(T_{sys})$ where $T_{sys}$ is the equivalent system noise temperature	$10 \log(T_{sys})$
$K_b$	Boltzmann constant	-228.6 dBW/Hz-K

The effective C/N0 (considering only pilots) is obtained from the actual C/N0 that the overall signal has (including pilots, data and other components). It is distinguished between the different types of signals (GPS L5, GPS L1C, Galileo-E1 and Galileo-E5a signals).

The SC antenna off-boresight angles to the NS satellites (obtained from the SC position and attitude, and the NS satellite positions) are considered to compute the gain in reception according to the antenna radiation diagram.

## GNSS Receiver Module (GRM)

This block implements a Raw Observable Generator (ROG) whose main objective is to generate fractional pseudoranges and frequency observables with the appropriate performance in a time-efficient way. The performance is determined by the type of received satellite signals and their corresponding parameters. As a result, this block generates observables that incorporate the effect of near-far interference and the noise in terms of acquisition probability and estimation accuracy. The ROG relies on a combination of analytical and numerical models that have been previously fitted to the results of sample-level simulations. But, the fact that the block avoids the generation of the observables using sample-level simulation reduces dramatically the execution time and allows for the analysis of long periods of time at a speed much faster than real-time. The high-level functionality of the GRM can be divided in two main parts:

- Data handling and configuration: This part handles the data present in the input file (from the SGM) for all time instants, satellites and antennas according to the chosen GRM configuration in order to select the signals from which the observables will be generated. The GRM can be configured to select the signal from the antenna with the highest C/N0 or from the antenna with the lowest near-far ratio (NFR). It also allows for enabling or disabling the near-far mitigation (which is a feature that at the same time has an impact on the effective NFR), and for setting global and per-phase C/N0 thresholds. Furthermore, for each mission phase, it is possible to let the receiver select the best correlation configuration based on the C/N0 or to force a given configuration.
- Equivalent C/N0 computation and generation of simulated observables: An equivalent C/N0 is computed starting from the C/N0 in the input file, which is corrected by the near-far equivalent degradation and other losses than have been computed to fit the analytical model to the simulations. Next, the equivalent C/N0 and NFR are used to obtain the acquisition and accuracy performance of the receiver for both types of observables using models matching the performance of the sample-level processing. Once the acquisition and accuracy performances (in terms of acquisition probability and standard deviation of the errors) have been computed, the observables are generated. Actually, it may also happen that the observables are not generated. This occurs when the C/N0 or NFR do not satisfy some minimum requirements or when, in spite of the fact that the C/N0 and NFR are adequate, the receiver suffers a miss-detection (and this occurs with a probability that is computed by this part of the module).

A detailed analysis based on sample-level simulations led to a selection three configurations for the coherent integration time and the non-coherent accumulations,  $\{T_{\text{coh}}, N_i\}$ , adequate to cover the range  $C/N_0$  values observed in the mission. These three configurations together with our recommended operation intervals are given by:

- 1)  $\{T_{\text{coh}}, N_i\}$  {1000 ms, 10}, for  $8 \leq C/N_0 \leq 10$  dBHz.
- 2)  $\{T_{\text{coh}}, N_i\}$  {500 ms, 10}, for  $10 \leq C/N_0 \leq 15$  dBHz.
- 3)  $\{T_{\text{coh}}, N_i\}$  {100 ms, 10}, for  $C/N_0 \geq 15$  dBHz.

It is important to remark that the  $C/N_0$  mentioned above is not the  $C/N_0$  of the received signal. Instead, it is the “effective”  $C/N_0$  corresponding to the pilot component of the GNSS signal under consideration.

A model was derived to compute the probability of detection ( $P_d$ ) based on the  $C/N_0$ , on the global probability of false alarm ( $P_{FA}$ ) and on the size of the time-frequency search region. It relies on the fact that the signal-free correlation results have a central chi-square distribution, while the signal-present correlation results have a non-central chi-square distribution. The model includes some acquisition losses around 2.5 dB, which are needed to match the simulation results. A key element of the model is the determination of the number of equivalent independent variables in search region since it

is an essential variable to link the per-cell probability of false alarm to the  $P_{FA}$ .

The model for the accuracy of the observables employs the theoretical bound (which is at the same time computed as the Crámer-Rao Bound of the estimation problem at hand, modified by a squaring-losses term for the case of the code-phase) corrected with some  $C/N_0$  losses, which have been obtained through extensive simulations. Fig. 9 shows the theoretical standard deviation (dashed line) and the actual standard deviation (solid line) for the code-phase (similar results have been obtained for the frequency, but they are not shown due to the lack of space). There is a gap between the theoretical and practical performance, and this effect can be modelled as a degradation of the actual  $C/N_0$ . This loss in terms of  $C/N_0$  is mainly due to bandwidth limitation, nonlinear effects and non-null bin size in the search region.

Table 1 summarizes the losses for all signals and observables. Therefore, before using the theoretical bounds for the measurement noise, the generator must correct the effective  $C/N_0$  (i.e. the  $C/N_0$  of the pilot component) by subtracting the  $C/N_0$  losses provided in the table, and the resulting  $C/N_0$  is the one to be used in the expression of theoretical bound. For  $C/N_0$  values different to those shown in Table 2, the losses can be obtained by means of quadratic interpolation.

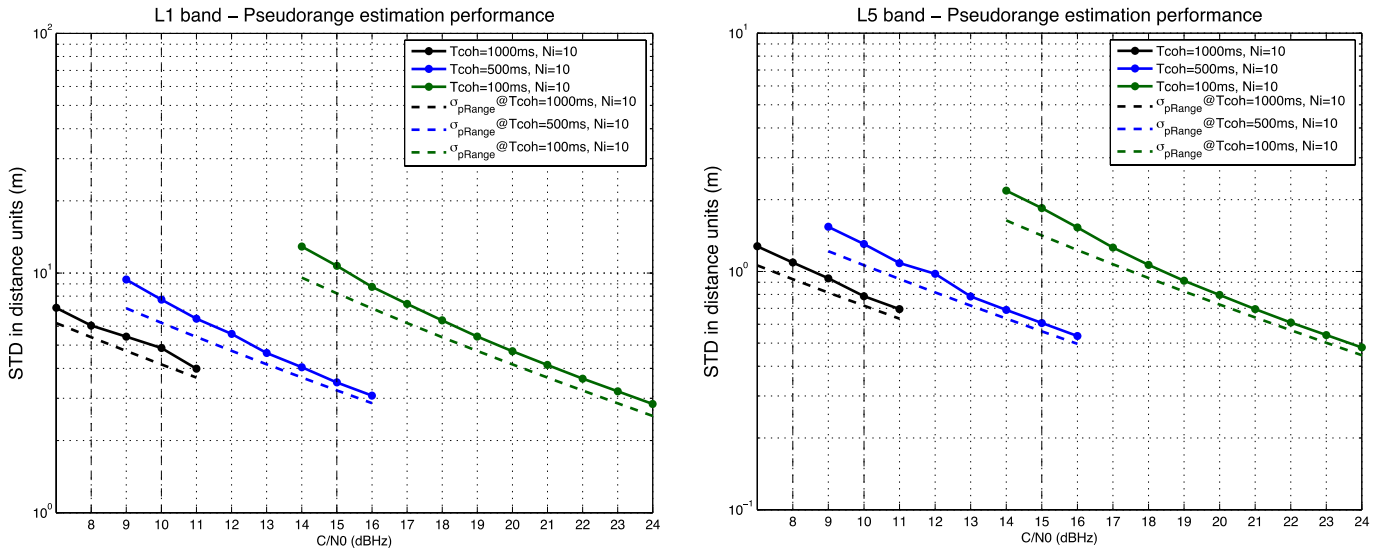


**Fig. 9: Comparison of the pseudorange estimation performance for Galileo E1C and E5A (solid lines) with the theoretical lower bound (dashed lines) as a function of the effective  $C/N_0$ , for bandwidths of 4 MHz (E1C) and 40 MHz (E5A).**

**Table 1:  $C/N_0$  losses experienced by the code-phase and frequency estimation algorithms for the different receiver configurations.**

$\{T_{\text{coh}}, N_i\}$	{1000 ms, 10}			{500 ms, 10}						{100 ms, 10}									
$C/N_0$ (dBHz)	8	9	10	10	11	12	13	14	15	15	16	17	18	19	20	21	22	23	$\geq 24$
<b><math>C/N_0</math> loss (dB) pRange@E1C, L1C</b>	1.3	1.1	1.0	1.5	1.3	1.0	1.0	1.0	1.0	2.3	1.8	1.6	1.4	1.2	1.1	1.05	1.0	1.0	1.0
<b><math>C/N_0</math> loss (dB) pRange@E5a,L5</b>	1.4	1.2	0.8	1.6	1.5	1.4	0.8	0.75	0.75	2.4	2.0	1.5	1.2	1.0	0.9	0.8	0.75	0.75	0.75
<b><math>C/N_0</math> loss (dB) vel@{E1C, L1, E5a, L5}</b>	2.3	2.1	1.8	2.8	2.5	2.0	2.0	2.0	2.0	4.5	3.5	3.0	2.5	2.2	2.0	1.7	1.4	1.25	1.0

The effect of near-far interference must also be accounted for in the acquisition and accuracy models. Again, sample-level simulations determine the effect of near-far interference. It is worth recalling that the NFR represents the ratio between the power of signal of interest and the power of all the interfering signals whose effect has not been eliminated using a NF mitigation technique. Moreover, the only signal whose NF contribution can be mitigated is the MGNSS signal since this signal can be designed to include only the pilot component (mitigation of the NF caused by data components is extremely difficult or even impossible when the C/N0 is so low that data cannot be detected). A threshold effect was observed; namely, when the NFR exceeds a given value (see Table 2), the correlation function is so distorted that acquisition becomes very unreliable and our recommendation is to discard the signal. In an intermediate region of NFR values, the effect of NF interference can be modelled as an equivalent C/N0 loss. For Galileo-E5a and GPS-L5, the losses amount only to a few tenths of dB, and they can be neglected with respect to other effects. For Galileo-E1C and GPS-L1C, losses due to NF are more noticeable and are represented in Table 3.

**Table 2: Summary of near-far effect on the different signals.**

	No significant losses	Transition region. NF mitigation is not necessary	Signal is recommended to be discarded unless NF can be mitigated
Galileo-E1C, GPS L1C	NFR < 12 dB	12 dB < NFR < 27 dB (CN0 losses given by the next table)	NFR > 27 dB
Galileo-E5a	NFR < 16 dB	16 dB < NFR < 31 dB (insignificant losses)	NFR > 31 dB
GPS-L5	NFR < 17 dB	17 dB < NFR < 32 dB (insignificant losses)	NFR > 32 dB

**Table 3: C/N0 losses (dB) in the E1C/L1C signals due to NF effects at intermediate NFR levels.**

NFR (dB)	NFR < 12	12 <= NFR < 15	15 <= NFR < 20	20 <= NFR < 25	25 <= NFR <= 27
Equivalent C/N0 loss (dB)	0	0.5	1.2	1.4	1.8

### Navigation Filter Module (NFM)

The Navigation Filter Module includes two main blocks:

- **Sensors:** This block contains the models of all the standard sensors and it is in charge of simulating the measurements of the standard sensors.
- **Navigation:** The navigation algorithm is composed by an EKF that hybridizes the standard sensors navigation solution with the GNSS measurements. The final outputs are the S/C estimated position and velocity.

The Sensors model implements the standard set of navigation sensors (not GNSS) according to the specifications and expected performances identified for the Moon GNSS reference scenario (see Table 4):

The Navigation block contains the algorithms for the attitude and trajectory determination. It implements an attitude filter and a translational filter in a tightly coupled architecture, allowing employing classical navigation filtering techniques, and at the same time the use every single measurement from GNSS. In the translational filter it is implemented a modified Extended Kalman Filter (EKF) that estimates the Spacecraft state using the propagation of the state and the measurements of the standard sensors. Then the GNSS re-correction block updates the state and the covariance matrix thanks to the hybridization with the available GNSS measurements. If more than 5 satellites are available (code ambiguity resolution), a stand-alone navigation with the GNSS signal is possible: both RLS method (Recursive Least Squares) and Peterson algorithm are implemented.

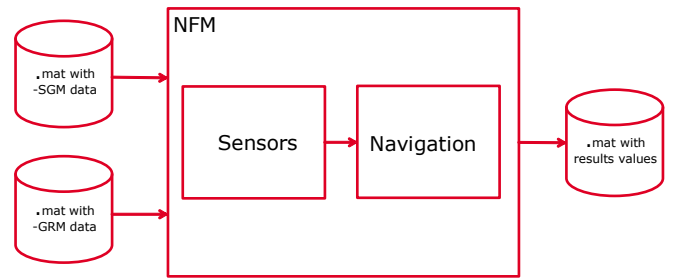


**Fig. 10: High level architecture of the Navigation Filter Module NFM**

**Table 4: Baseline standard sensors (not GNSS) for the different scenario phases**

Scenario phase	Sensors used in Attitude Dynamic	Sensors used in Translational Dynamic
LTO	-Gyros -Star Tracker	-Accelerometers -Ground tracking (when available) -Orbital Propagator
LLO	-Gyros -Star Tracker	-Accelerometers -Ground tracking (when available) -Orbital Propagator
COASTING	-Gyros -Star Tracker	-Accelerometers -Ground tracking (when available) -Orbital Propagator -Optical camera
D&L	-Gyros -Star Tracker (when available)	-Accelerometers -Ground tracking (when available) -Orbital Propagator -Optical camera -Laser Altimeter

### SIMULATION RESULTS

The test plan has been designed to be representative of a real Moon-GNSS mission covering all the mission phases representative of the real mission conditions in terms of dynamics and signal disturbances. For this purpose, the following parameters have been identified:

- **Mission phases:** 8 mission phases have been identified and presented in the Moon-GNSS scenario definition.
- **Signals:** two different frequency bands (L1, L5) have been considered.

- Presence of GNSS signals: the analysis includes navigation with and without GNSS signals. If the GNSS signals are not present the navigation considers only the standard sensors for the Lunar Lander mission (see Table 4).
- Presence of MGNSS: Two scenarios are considered: additional GNSS-like source at the vicinity of the Moon (MGNSS) and no additional GNSS-like source at the vicinity of the Moon. During the test campaign the optimum MGNSS constellation has been analyzed. Dedicated test cases have been performed to select which is the best MGNSS approach (adaptive power or high power).
- Ground Tracking measurements update period: thanks to the GNSS measurements it should be possible to improve the Spacecraft state estimation and to reduce the Ground Tracking update frequency (from once per hour which is the standard case, up to once per day).
- GNSS receiver module parameters: the integration type may change or remain fixed according to external constraints; a sensibility analysis of the window uncertainties for the signal acquisition is performed; the best strategy to choose the receiving antenna for each signal is evaluated.

The test cases cover the following areas:

- Frequency band selection for the GNSS signals (L1 or L5).
- Optimum MGNSS transmission power selection (near-far effect).
- Evaluation of the performances with reduced frequency of ground tracking measurements updates.
- Evaluation of the best strategy for the selection of the receiving antenna.
- The fifth case aims at performing the sensibility analysis of the GNSS receiver to the given uncertainty window in position and velocity.
- The rest of the cases evaluate the performances of the Moon-GNSS receiver covering all the mission phases and under different conditions.

The Moon mission scenario is very challenging for the GNSS signals acquisition. Due to the large propagation distances, the signal arrives with low  $C/N_0$  values. In order to acquire these attenuated signals, high-sensitivity algorithms similar to the ones used for reception indoor can be used in the receiver. An efficient algorithm to implement long correlations (combining coherent and non-coherent integrations) has been proposed. Three combinations of coherent and non-coherent integrations have been proposed to cover the range of  $C/N_0$  values where the receiver has to operate.

Moreover, the receiver can also employ two operating modes consisting in:

- Fixing the integration time to a value for all the signals received during a mission phase
- Selecting the integration time as a function of the expected  $C/N_0$

It is clear that to settle the receiver in a configuration where the integration time is fixed simplifies considerably its management. The configurations that integrate 1 second (10 non-coherent integrations of 100ms) and 5 seconds (10 non-coherent integrations of 500 ms) facilitate implementation. Moreover, it has been corroborated that with only these two configurations it is possible to satisfy the overall mission requirements, avoiding the configuration of 10 seconds (10 non-coherent integrations of 1000 ms), which is very challenging from an implementation point of view.

This study has carefully analyzed all the test cases that were considered interesting in order to evaluate the hybrid, standard and stand-alone GNSS navigation performances. The “standard” navigation algorithm is an EKF that considers the nominal sensors for the Lunar Lander mission, while the hybridization filter consists in an EKF with a second update (LS) that takes into account the GNSS measurements. Also a stand-alone GNSS navigation has been considered, in order to evaluate the possibility to avoid/limit the adoption of standard sensors. During the lunar phases before Moon landing because of the nominal attitude of the Spacecraft and because of the Moon blinding effect, the hybrid navigation accuracy is of the same order of magnitude of the one obtained with the standard navigation (Fig. 11). The analysis showed that when relative sensors such as Optical camera and Laser altimeter are available, the navigation accuracy does not significantly improve with the GNSS measurements. Indeed, during these final phases before Moon landing only few weak signals are received, so that the accuracy of the GNSS measurements is far worse than the one obtained using the relative sensors. The study of the Surface Operation phase showed that even if good results can be achieved using a stand-alone GNSS navigation, the accuracy is not enough to consider these measurements for rover navigation (Fig. 12).

The best results are obtained considering the signal transmitted by the MGNSS, a GNSS satellite orbiting around the Moon. Indeed, this added measurement significantly increases the precision of the state estimation, especially if its trajectory is properly designed to reduce the DOP factor. It is also interesting to appreciate how the MGNSS can improve the navigation estimation of the landing site (see Fig. 14). The analysis deeply investigated the reasons why a single measurement from the MGNSS strongly affects the navigation performances. The results of the tests show that the improvement is mainly caused by the reduction of the DOP factor, and not by the emitting power of the MGNSS. The most interesting results have been obtained during the LTO phase tests (see Fig. 13). Indeed, thanks to the nominal attitude of the Spacecraft, it is possible to receive a high number of GNSS signals adopting only one high gain antenna even with a high  $C/N_0$  minimum threshold of 12 dBHz. The stand-alone GNSS navigation performances are very good at the beginning of the orbit (close to the Earth) and reach approximately the accuracy

of the standard navigation at the end (close to the Moon). The hybrid navigation performances are even better, even with a reduced ground tracking updating frequency. It is interesting to notice the effect of the MGNSS measurement during the LTO phase. When it is correctly acquired, the navigation solution accuracy becomes higher than the one obtained with the ground tracking. To summarize, the main advantages of the GNSS measurements processing are mostly visible during the LTO phase:

- High accuracy of the hybrid navigation estimation;
- Operations from ground frequency can be reduced up to once per day (in a 5 days phase this means having 5 ground tracking updates instead of more than one hundred);
- Especially in the first part of the orbit (up to GEO), the hybrid navigation precision is significantly higher than the one obtained using the inertial navigation, the on-board propagation and an hourly ground tracking update.

It is important to highlight that the accuracy obtained using only the GNSS satellites from Earth (GPS and Galileo constellation) is enough to respect the mission requirements during this LTO phase. This means that the conclusions above are still valid even without the MGNSS satellite orbiting around the Moon and mounting only one High Gain Antenna on the Spacecraft.

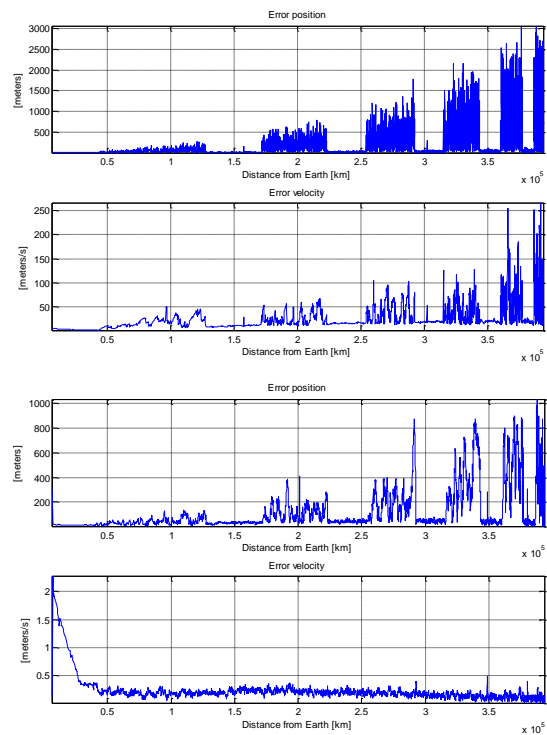


**Fig. 13: Absolute knowledge position and velocity errors (ECI). GNSS stand-alone navigation (left), hybrid GNSS + standard sensors navigation (right) – LTO phase**

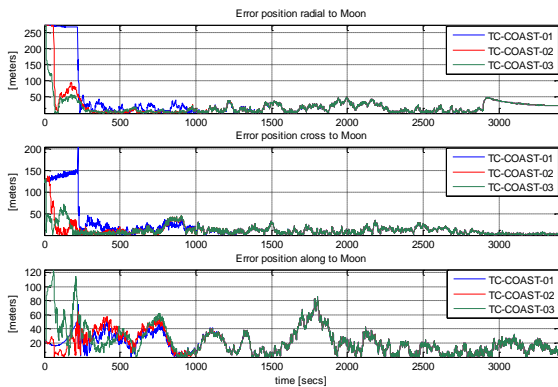


**Fig. 11: Absolute knowledge position and velocity error (ACRM). Standard navigation (blue), hybrid navigation EGNSS (red), hybrid navigation with EGNSS + MGNSS (green) – Coasting phase**

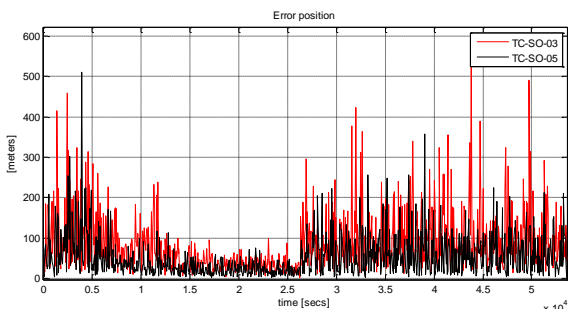


**Fig. 12: Absolute knowledge position error (ECI). Hybrid navigation with EGNSS + MGNSS, L1 frequency (red), L5 frequency (black) – Surface Operation phase**

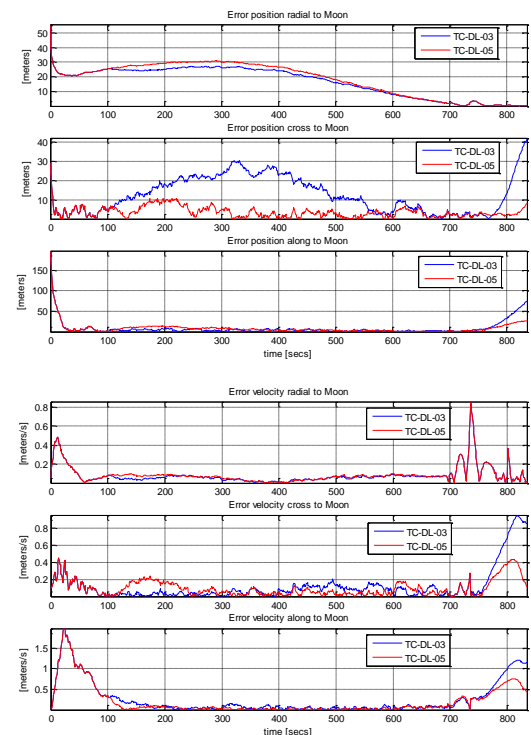


**Fig. 14: Absolute knowledge position and velocity error (ACRM). Standard navigation (blue), hybrid navigation with a dedicated MGNSS orbit (red) – D&L phase**

## CONCLUSIONS

During the Moon-GNSS activity, an analysis and identification of the navigation receiver requirements for the upcoming lunar exploration missions has been performed.

The first task has been to define the Moon-GNSS scenario to be used as reference for the GNSS receiver and the later hybridization with other sensors. An extensive Moon-GNSS scenario analysis has been performed in order to provide with the due inputs for the derivation of the Moon-GNSS navigation receiver requirements, and for the definition the GNSS receiver module architecture and algorithms (weak signal processing, filtering and navigation).

The architecture of the GNSS receiver module has been proposed, based on an open-loop configuration that generates the code-phase and frequency estimates. It has been implemented to be compatible with GPS and Galileo signals, both with pilot and data components. Furthermore, it is designed to achieve the low levels of sensitivity required for indoor applications. It is based on the ESA patented "Double-FFT Method" for an efficient implementation all these techniques.

A PoC simulator has been developed, and its main components are described in detail. A test campaign has been performed representative of a real Moon-GNSS mission covering all the mission phases representative of the real mission conditions in terms of dynamics and signal disturbances. The functional and performance results have been presented.

The Moon-GNSS main conclusions are that a specifically designed GNSS receiver should be capable of receiving and processing GNSS signals coming from Earth during a lunar mission, and that the resulting GNSS measurements can be used in a tight coupling hybridization filter to generally improve the "standard" navigation performances.

## REFERENCES

- [1] The European Lunar Lander Mission. Alain Pradier. ASTRA., 12th April 2011.
- [2] L. Winternitz, M. Moreau, G. Boegner, S. Sirotzky, "Navigator GPS Receiver for Fast Acquisition and Weak Space Applications", ION GNSS 2004.
- [3] D. Kubrak, G. Seco-Granados, J. A. Lopez-Salcedo, J. L. Vicario, E. Aguado, "TN2: Technological challenges and state-of-the-art indoor positioning survey document" DINGPOS project, Oct 2007.
- [4] M. Monnerat, D. Kubrak, Y. Capelle, G. Seco-Granados, J. A. Lopez-Salcedo, J. L. Vicario, I. Fernández, A. Consoli, T. Ferreira, "TN3: Platform architectural design and performance justification", DINGPOS project, Nov 2007.
- [5] G. Seco-Granados, J.A. Lopez-Salcedo, D. Jimenez-Banos, G. Lopez-Risueno, "Challenges in Indoor Global Navigation Satellite Systems: Unveiling its core features in signal processing," Signal Processing Magazine, IEEE, vol.29, no.2, pp.108,131, March 2012.

- [6] J. Roselló, P. Silvestrin, R. Weigand, S. d'Addio. A. García Rodríguez, G. López Risueño, "Next Generation of ESA's GNSS Receivers for Earth Observation Satellites", NAVITEC, 2012.
- [7] P.J. Buist, G.J. Vollmuller, "On-board FFT Data Processing for GNSS Reflectometry", ION ITM, 2013.